Vortex formation by active agents as a model for *Daphnia* swarming

Jürgen Vollmer,[1,*] Attila Gergely Vegh,[2] Christoph Lange,[1] and Bruno Eckhardt[1]
[1]*Fachbereich Physik, Philipps-Universität Marburg, Renthof 6, D-35032 Marburg, Germany*
[2]*Department of Physics, Babes-Bolyai University, Strada Mihail Kogalniceanu 1, RO–3400 Cluj Napoca, Romania*
(Received 5 December 2005; revised manuscript received 10 April 2006; published 30 June 2006)

We propose a self-propelled particle model for the swarming of *Daphnia* that takes into account mutual repulsion and attraction to a center. Surprisingly, a vortex is formed only for an intermediate strength of propulsion. The phase diagram and the transitions between states with and without a vortex are analyzed, and the nature of the phase boundaries is discussed based on a linear stability analysis of the motion of individual swimmers. This allows us to identify various key parameters determining the characteristic features of the collective motion.

DOI: 10.1103/PhysRevE.73.061924 PACS number(s): 87.19.St, 05.65.+b, 47.32.cd, 64.60.−i

I. INTRODUCTION

Phenomena in the biological realm [1] such as the colony organization of microorganisms [2], the schooling of fish and birds [3–6], the swarming of small insects [7,8], or the herding of wild animals [9] show dynamical behavior that is tantalizingly similar to the well understood order-disorder transitions in equilibrium physics [10,11]. Both groups of systems can show a change from a disordered state, where every constituent moves more or less independently, to ordered circular or directed motion with obvious correlations between neighbors. In contrast to the situation with equilibrium systems the modeling of groups of living organisms faces the additional challenge that there are no first-principles descriptions, no Hamiltonians, and no equilibrium ensembles. Despite these uncertainties it has been possible to identify a few key elements in the models required for the formation of the ordered state [3,12–22]. For instance, Vicsek and co-workers [12,13] attribute the emergence of ordered motion in a flock to the tendency of neighboring animals to align their velocities. Toner and Tu [14,15] emphasize the similarity between this interaction and the spin-spin interaction to arrive at a model for swarming that is closely related to *X-Y* models in statistical physics. Levine *et al.* [17] consider "multiagent" models based on the dynamics of individual agents. They obtain aggregation from attractive interactions and the tendency of the agents to move with a finite velocity. Chaté *et al.* [23,24] worked out the analogies between aggregation in these type of models and liquid-gas phase transitions. Mikhailov and co-workers [25,26] worked out noise-induced transitions to ordered motion in multiagent models with long-range attraction. All these models are spatially homogeneous with long-range attractions, and most of them have a stochastic forcing built into them.

In contrast, our emphasis in the present paper is on situations where the transition to an ordered state is induced by externally imposed heterogeneities. Specifically, we will study situations where a localized attractive stimulus triggers the formation of a macroscopic vortex motion. In [19,21,27–29] this problem was discussed using active Brownian particles in a confining potential. In the present study we complement this work by a discussion of the transitions in a deterministic model of active agents which interact by short-range repulsive forces.

The motivation for our studies derives from observations of swirling motion in groups of *Daphnia Magna* in Frank Moss' laboratory [30–32]. The vortex formation is induced by sending a light beam vertically into the water. The *Daphnia* are attracted to visible light. They enter into a swirling motion, while more *Daphnia* from the surrounding area are attracted. We will show here that a model that contains an active motion, a weak attractive force towards the light beam, and mutual repulsion between the *Daphnia* is sufficient to explain the vortex formation. However, if the active motion becomes either too weak or too persistent, the vortex disappears. In addition, we show that the vortex formation has self-stabilizing features. Fluctuations of the direction of motion are much reduced compared to the nonvortex state.

Even though the study is motivated by observations on *Daphnia* [30–32], we do not aim for a detailed model of their swimming, i.e., we do not consider their nonspherical shapes, the details of the motion of their appendages, or their swimming protocol with its active and passive segments. Rather we aim for a minimal model that allows us to reproduce salient features of the experiments. To underline this emphasis we will, therefore, refer to the objects we model as "swimmers": they are active and move in a smooth, deterministic manner. Our study confirms the significance of the active propulsion for the formation of the vortex, and allows us to compute some quantities that can then be compared to observations on *Daphnia Magna*.

In Sec. II the dynamics and the various interactions are introduced and the stability of circular motion is studied. In Sec. III the emergence of vortices as a function of the system parameters and the swimmer number is studied and a phase diagram is presented. The main results are summarized in Sec. IV.

II. EQUATIONS OF MOTION

Daphnia swim by paddling with their front legs. Individual *Daphnia* alternate between phases of rapid swimming and periods of rest. Their speed is about a few mm/s relative

*Electronic address: juergen.vollmer@physik.uni-marburg.de

to the surrounding water. While it is conceivable that they could steer by varying the strength of paddling on either side, they do not seem to explore that option: during swimming their motion is along fairly straight line segments. The variations in direction between consecutive swimming segments come from stochastic reorientations and are not very big: on times much longer than these swimming intervals the tracks of *Daphnia* look fairly smooth. A stochastic hopping model similar to the ones used by Berg [33] for *E. coli* could be used to model this behavior, but only at the cost of additional parameters. Hence, we chose to work with a continuum model.

A. Continuum Model

In a continuum model the equations of motion are stated as differential equations for the position $\mathbf{x}$ and the velocity $\mathbf{v}$ of the swimmers. The position changes according to

$$\dot{\mathbf{x}} = \mathbf{v}, \tag{1a}$$

where $\mathbf{v}$ is the speed of the swimmer relative to the water, which is assumed to be at rest for the purpose of the present study. The speed, in turn, changes according to

$$\dot{\mathbf{v}} = \gamma_0\left(1 - \frac{\mathbf{v}^2}{v_0^2}\right)\mathbf{v} + \mathbf{f}. \tag{1b}$$

The first term describes the self-propulsion and reflects the swimmers' efforts to keep the speed close to a preferred speed v_0. The efforts are characterized by a relaxation rate γ_0 or a relaxation time $1/\gamma_0$. For small γ_0 the force restoring the preferred velocity v_0 is only weak, and regular Newtonian dynamics are obtained. On the other hand, for large γ_0 essentially only the direction of $\mathbf{v}$ but not its magnitude can change.

The second term in (1b) contains all external influences: attraction to the light center, avoidance maneuvers with other swimmers, and possible alignment effects between neighboring swimmers. Various choices to implement self-propulsion and their physical interpretation have been surveyed elsewhere [34,35]. The analysis of the consequences of different choices for $\mathbf{f}$ will be an integral part of the present study.

The equations can be nondimensionalized by introducing a scale for the velocity (for which v_0 is the natural choice), and a length scale ℓ, which we take to be about twice the diameter of the swimmers (cf. Sec. II E) [37].

Except for the absence of a stochastic forcing, Eqs. (1) are the active model studied by Ebeling *et al.* [18–21] and Levine *et al.* [17]. Further differences come from the choice of potentials.

B. Swimmers in a harmonic potential

Ebeling *et al.* [18–21] use a harmonic force for the attraction to the center,

$$\mathbf{f} = -\nabla V \tag{2}$$

with

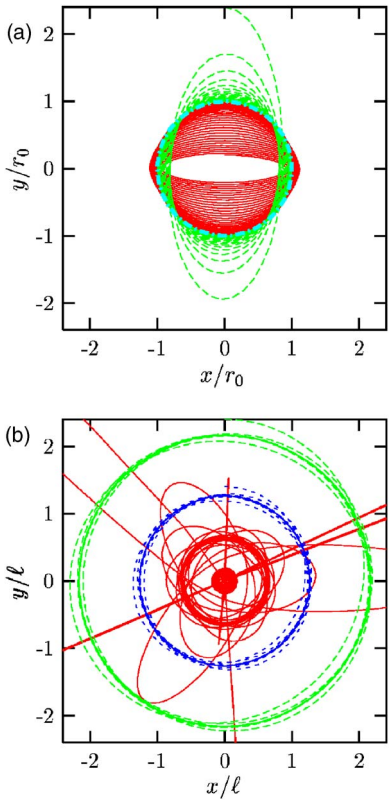

FIG. 1. (Color online) Evolution of trajectories for $\gamma=0.05$ that all start with velocity $\mathbf{v}_{\text{ini}}=(0.9,0)$ at $x_{\text{ini}}=0$. (a) In the harmonic potential all trajectories converge to a motion along the unit circle [$y_{\text{ini}}=0.2$ (solid, red), $y_{\text{ini}}=2.4$ (long dashed, green)]. (b) In a logarithmic potential the asymptotic motion can be a cycle with any radius [$y_{\text{ini}}=0.2$ (solid, red), $y_{\text{ini}}=1.4$ (short dashed, blue), $y_{\text{ini}}=2.4$ (dashed, green)].

$$V_{\text{harm}}(\mathbf{x}) = \frac{\omega_0^2}{2}\mathbf{x}^2, \tag{3}$$

where ω characterizes the strength of the harmonic potential. In dimensionless units the evolution depends only on the control parameters $\gamma \equiv \gamma_0/\omega$ and $\omega \equiv \omega_0\ell/v_0$. The equations of motion for a single swimmer then take the form

$$\dot{\mathbf{x}} = \mathbf{v}, \tag{4a}$$

$$\dot{\mathbf{v}} = \gamma(1-\mathbf{v}^2)\mathbf{v} - \omega^2\mathbf{x}. \tag{4b}$$

This system of equations has one trivial solution, where the swimmer is at rest in the center, $\mathbf{v}=0$ and $\mathbf{x}=0$. Since $\gamma>0$ this solution is unstable. There are further unstable solutions with tracks oscillating along lines through the origin. Finally, there are two circular motions with $|\mathbf{x}|=|\mathbf{v}|=1$ (cf. Fig. 1), which differ only in the sense of orientation around the center. The radius r_0 of the circular motion is selected by a balance between centrifugal forces, $\sim v_0^2/r_0$, and the trapping force, $\sim\omega^2 r_0$. This leads to $r_0=v_0/\omega_0$ such that $r_* \equiv r_0/\ell = v_0/\omega_0\ell = \omega^{-1}$ in dimensionless units.

The trajectory of single swimmers are shown in Fig. 1(a). Irrespective of the choice of initial conditions (and of ℓ, ω) they approach a circular motion of radius r_0. Indeed, these

solutions are globally stable: typical initial conditions are attracted to the circular motion. Analytically this is best verified in polar coordinates, where the $2d$ vectors $\mathbf{x}$ and $\mathbf{v}$ are represented by complex variables:

$$\mathbf{x}(t) = r(t)e^{i\phi(t)}, \tag{5a}$$

$$\mathbf{v}(t) = iu(t)e^{i\theta(t)}. \tag{5b}$$

The equations of motion (4) become

$$\dot{r} = -u\sin(\theta-\phi), \tag{6a}$$

$$\dot{u} = \gamma(1-u^2)u + \omega^2 r\sin(\theta-\phi), \tag{6b}$$

$$\dot{\phi} = \frac{u}{r}(\theta-\phi), \tag{6c}$$

$$\dot{\theta} = \frac{\omega^2 r}{u}\cos(\theta-\phi). \tag{6d}$$

Only the three variables r, u, and the angle difference $\psi=\theta-\phi$ are dynamically coupled, the mean angle $\tilde{\psi}=\theta+\phi$ follows by integration once the other three are known.

Linearizing the equations of motion for the three relevant variables around the circular motion $\psi=0$, $u=1$ and $r_*=\omega^{-1}$ yields

$$\frac{d}{dt}\delta r = -\delta\psi, \tag{7a}$$

$$\frac{d}{dt}\delta u = -2\gamma\delta u + r_*^{-1}\delta\psi, \tag{7b}$$

$$\frac{d}{dt}\delta\psi = 2r_*^{-2}\delta r - 2r_*^{-1}\delta u. \tag{7c}$$

For $\gamma>0$ there is a real eigenvalue λ_0 obeying the implicit equation $\gamma r_*=-\lambda_0 r_*[(\lambda_0 r_*)^2+4]/[2(\lambda_0 r_*)^2+4]$ (filled circles ● in Fig. 2), and two complex-conjugated eigenvalues $\lambda_\pm$ with real parts $-\lambda_0/2-\gamma$ (open circles ○ in Fig. 2). The real parts of all three eigenvalues are always negative such that the circular motions are always stable. Indeed, the circular motion is not only locally, but also globally stable—irrespective of the initial conditions a swimmer will settle down to a clockwise or counterclockwise circular motion, both stable limit cycles in phase space.

On the other hand, the relaxation rates towards the limit cycles tend to vanish for small as well as for large γ. For small γ the real eigenvalue λ_0 vanishes like $\lambda_0\sim-\gamma$, and the real part of the complex eigenvalues like $\mathrm{Re}(\lambda_\pm)\sim-\gamma/2$. For large γ the real eigenvalue continues to grow as $\lambda_0\sim-2\gamma$, while the real part of the complex eigenvalues vanishes as $\mathrm{Re}(\lambda_\pm)\sim-(2\gamma r_*^2)^2$.

The main feature of motion in the harmonic potential is that the swimmers select one of the two circular trajectories for the swarm. If Eq. (4) is augmented with the mutual repulsion [see Eq. (15) below] all swimmers cluster in an annulus rather than a vortex. If random perturbations are added, as in [17,19,34], the tracks will show some more spreading around the limit cycle, but the overall impression will still be that of an annulus in which the swimmers are trapped. Moreover, the decrease of stability of the limit cycle for both small and large γ suggests that for interacting swimmers the ordered motion might only be possible for a limited range of γ values.

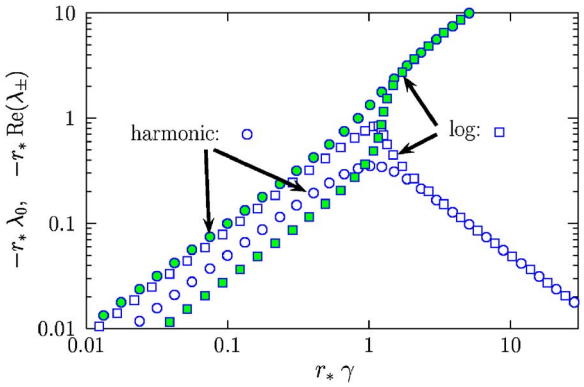

FIG. 2. (Color online) The γ dependence of the absolute values of the real eigenvalue (filled symbols) and of the real parts of complex eigenvalues (open symbols) of the stability matrix for circular motion. For the harmonic potential (○) there are always one real and two complex eigenvalues, and this also holds for the truncated logarithmic potential with $\sigma=1.1$ (□). The radius r_* of the considered circular orbit only enters the stability analysis as a factor in the time unit. It disappears when time is specified in multiples of the revolution time around the origin rather than by ℓ/u_0. In all cases the real parts of the eigenvalues are negative.

C. Swimmers in a logarithmic potential

Interactions that admit a wide range of circular orbits have to meet the condition that the attractive force balances the centrifugal forces over a wider range of radii. Due to their selfpropulsion, the swimmers move with a velocity close to v_0. Therefore, their angular velocity is about $\Omega(r)=v_0/r$ and the centrifugal force falls off as $\Omega^2 r=v_0^2/r$. Consequently, a neutrally balancing attracting force has to fall off as v_0^2/r as well. The corresponding potential increases only logarithmically,

$$V_{\log}(\mathbf{x}) = \frac{v_0^2}{2}\ln\frac{\mathbf{x}^2}{\ell^2}. \tag{8}$$

In terms of the dimensionless units defined above the equations of motion then attain the form

$$\dot{\mathbf{x}} = \mathbf{v}, \tag{9a}$$

$$\dot{\mathbf{v}} = \gamma(1-\mathbf{v}^2)\mathbf{v} - \frac{\mathbf{x}}{r^2}, \tag{9b}$$

where the radius $r=|\mathbf{x}|$. Note that the logarithmic potential does not have a free strength parameter and does not select a length scale. As a consequence, for the logarithmic potential *all* circular orbits are neutrally stable. Writing Eqs. (9) in polar coordinates and linearizing around a circular orbit of

radius r_* yields for the motion of individual swimmers

$$\frac{d}{dt}\delta r = -\delta\psi, \tag{10a}$$

$$\frac{d}{dt}\delta u = -2\gamma\delta u + r_*^{-1}\delta\psi, \tag{10b}$$

$$\frac{d}{dt}\delta\psi = -2r_*^{-1}\delta u. \tag{10c}$$

This set of equations differs from Eqs. (7) only in the absence of the term $2r_*^{-2}\delta r$ in the equation for $\frac{\mathrm{d}}{\mathrm{d}t}\delta\psi$. As a consequence, there is one neutral direction, changing δr, and two stable eigenvalues $-\gamma\pm[(\gamma r_*)^2-2]^{1/2}/r_*$ characterizing the velocity and phase difference. Accordingly, the asymptotic motions are circles of radii determined by the initial conditions [Fig. 1(b)].

The restoring forces to the motion on a circle are weak for both small γ, where the total energy becomes approximately conserved and the eigenvalues are complex with real part $-\gamma$, as well as for large γ, where the system essentially becomes overdamped with eigenvalues close to -2γ and $-(2\gamma r_*^2)^{-1}$. Again, this suggests that perturbations, such as interactions with other swimmers, can destabilize the circular motion for both small *and* large γ.

D. Truncated logarithmic potential

Even in the absence of interactions with other swimmers there are large irregularly looking excursions of the trajectory starting at $y_{\mathrm{ini}}=0.2$ [the solid line in Fig. 1(b)]. They are caused by a close approach of the $1/r$ singularity of the logarithmic potential. This singularity is not only numerically inconvenient but also physically implausible since it can lead to trapping of swimmers in the singularity. We therefore cut off the potential at a radius ϵ and introduce a dimensionless strength σ that will always be of order one,

$$V_{\mathrm{trunc}}(\mathbf{x}) = \frac{\sigma^2 v_0^2}{2}\ln\left(1+\frac{\mathbf{x}^2}{\epsilon^2}\right). \tag{11}$$

The dimensionless equations of motion become

$$\dot{\mathbf{x}} = \mathbf{v}, \tag{12a}$$

$$\dot{\mathbf{v}} = \gamma(1-\mathbf{v}^2)\mathbf{v} - \frac{\sigma^2\mathbf{x}}{r^2+\epsilon^2}. \tag{12b}$$

For $r \lesssim \epsilon$ the swimmers feel a harmonic force of strength $\omega = \sigma/\epsilon$, which is too weak to balance the centrifugal term $\propto 1/\epsilon^2$; they move outward. At larger distances r from the center the logarithmic potential is recovered up to corrections that are smaller than the leading order term by a factor $(\epsilon/r)^2$. Choosing σ slightly larger than unity introduces a weak inward drift, while $\sigma \leqslant 1$ leads to an outward spiral. We will always choose $\sigma=1.1$.

The linearized equations of motion in the vicinity of the asymptotic circular motion are

$$\frac{d}{dt}\delta r = -\delta\psi, \tag{13a}$$

$$\frac{d}{dt}\delta u = -2\gamma\delta u + \frac{1}{r_*}\delta\psi, \tag{13b}$$

$$\frac{d}{dt}\delta\psi = \frac{2}{r_*^2}(1-\sigma^{-2})\delta r - 2\frac{1}{r_*}\delta u. \tag{13c}$$

For $\sigma=1$ one recovers the case (10) and for $\sigma\to\infty$ the harmonic one (7). The eigenvalues describing the stability of the resulting limiting orbit are shown in Fig. 2(■,□). The real eigenvalue λ_0 obeys the implicit equation $\gamma r_* = -\lambda_0 r_*[(\lambda_0 r_*)^2+4-2/\sigma^2]/[2(\lambda_0 r_*)^2+4-4/\sigma^2]$ (filled boxes ■), and the two complex-conjugated eigenvalues have real parts $\mathrm{Re}(\lambda_\pm)=-\lambda_0/2-\gamma$ (open boxes □). One notes that again restoring forces are weak for both small and large γ. In the former case the (real parts of the) eigenvalues approach $-2\gamma(\sigma^2-1)/(2\sigma^2-1)$ and $-\gamma\sigma^2/(2\sigma^2-1)$, respectively. For large γ the system is again overdamped with eigenvalues close to -2γ and $-(2\gamma r_*^2)^{-1}$. In contrast to the harmonic case the circular orbit appears to be less stable, however, in the logarithmic case.

E. Hard-core interactions and dimensionless units

Daphnia tend to avoid each other when approaching each other closer than about twice their diameter [36]. For simulations with several *Daphnia* we have to model their mutual repulsion. This will be taken into account by strong, essentially hard-core repulsions which appear when the distance D between two swimmers falls below the *interaction distance* D_{I}. The smooth representation of this short-range repulsion is modeled after the repulsive part of a Lennard-Jones potential,

$$V_{\mathrm{I}}(D) = \nu\left[\left(\frac{D_{\mathrm{I}}}{D}\right)^{12} - 2\left(\frac{D_{\mathrm{I}}}{D}\right)^{6}\right]. \tag{14}$$

For swimmers that approach each other within a distance D_{I} this introduces a force

$$-\nabla V_{\mathrm{I}}(\mathbf{D}) = 12\nu\left[\left(\frac{D_I}{D}\right)^{12} - \left(\frac{D_{\mathrm{I}}}{D}\right)^{6}\right]\frac{\mathbf{D}}{D^2} \tag{15}$$

in the equations of motion, which is directed along the relative position $\mathbf{D}$ of the swimmers.

The short-range repulsion introduces a natural length scale, the interaction distance D_{I}, which is of the order of twice the diameter of the swimmers. Henceforth, we will measure all length scales in units of the distance $\ell \equiv D_{\mathrm{I}}$, and velocities in units of v_0.

F. Confinement

The logarithmic potentials are characterized by their tendency to stabilize circular motions. Radially outward motion is not stabilized, however, since the energy reservoir of the swimmers allows them to maintain their speed while at the same time the redirecting force towards the center becomes

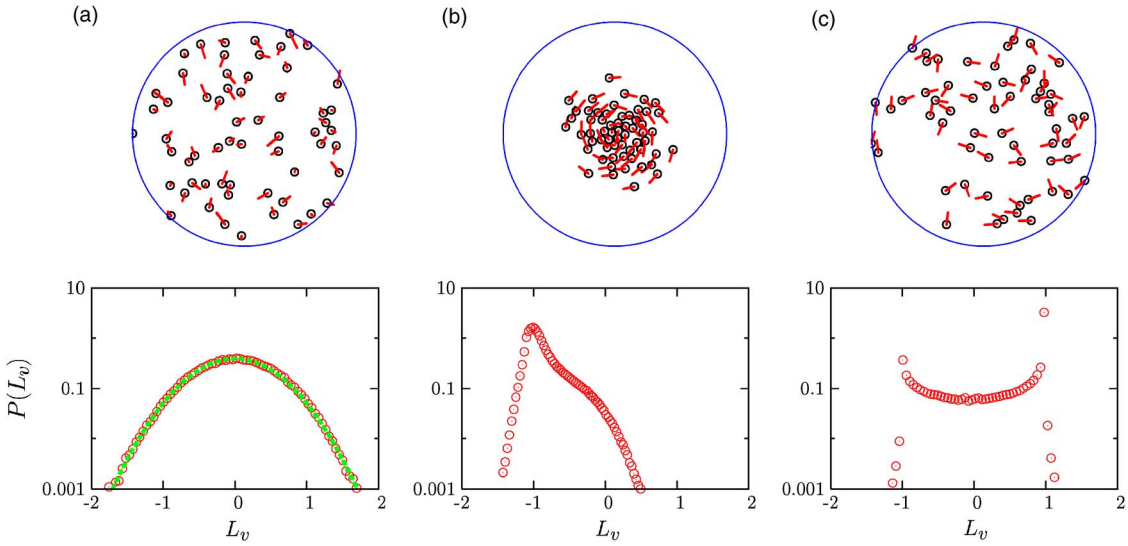

FIG. 3. (Color online) Snapshots of the motion of $N=60$ swimmers in a logarithmic potential (top) together with the corresponding histograms for L_v (bottom). Swimmers are represented by open circles. The tick marks indicate the direction of the motion, and their length is proportional to their velocity. (a) For $\gamma=0.001$ the swimmers access all available space, and their velocity distribution amounts to a Maxwell distribution with variance 0.5 (dashed line). (b) For $\gamma=0.1$ one observes a fairly densely packed vortex with a very narrow velocity distribution peaked around $L_v=-1$. (c) For $\gamma=10$ the swimmers again access all available space. However, they have a strong preference for azimuthal motion leading to a bimodal velocity distribution with peaks at $L_v=\pm 1$.

weaker. The system is therefore unbounded in that swimmers can escape to infinity. This seems to be in accord with experiments [36], where the vortex forms in a fraction of the container with some residual *Daphnia* concentration surrounding it and with *Daphnia* sometimes leaving the cluster.

An easy way to deal with this unboundedness of motion is to introduce a circular bounding wall. At the wall one has the choice between different boundary conditions: (i) a deterministic reflection which reverses just the radial component of the velocity; (ii) letting the swimmers continue their tracks by reentering from the opposite side of the wall while keeping their velocity; or (iii) a stochastic boundary condition, where every swimmer that is about to escape is reinjected at some place in the vicinity of the wall with an inward pointing velocity. While the latter condition is more representative of a surrounding reservoir of swimmers, simulations with other types of boundary conditions do not show states with noticeably different statistical properties. On the other hand, the best numerical performance was obtained when implementing the walls by subjecting swimmers to a very strong confining harmonic potential once their distance from the center exceeds 14 (i.e., 14 short-range interaction distances D_{I}). In all simulations discussed in the following this latter choice has therefore been adopted.

III. VORTEX FORMATION

A. Choice of parameters

The choice of the preferred velocity v_0 of the swimmers as velocity scale and their interaction distance D_{I} as a measure of length fixes the time scale to be $\tau=D_{\mathrm{I}}/v_0$. For *Daphnia* of diameter 1 mm moving with velocities of 1 mm/s this corresponds to about 1 s.

The relaxation rate of the velocity for *Daphnia* is near $\gamma=0.4$, implying that the preferred velocity is restored after a travel distance of about five diameters. This is in fair agreement with experimental observations, and it also allows for a noticeable short-time increase or decrease of velocity when the swimmers try to separate in an effort to avoid a collision.

The cutoff of the logarithmic potential is identified with the typical interaction distance between swimmers, $\epsilon=D_{\mathrm{I}}=1$ so that the cutoff mimics the fact that the force disappears once a swimmer sits right in the center of the system. Otherwise, the logarithmic force could induce a very rapid spinning of swimmers around their own axis, which is clearly not meaningful for the modeling of the *Daphnia*.

Finally, for convenience, we choose $\nu=1/12$ in the definition (15) of the force. Other values for ν influence the details of binary collisions and hence alter the trajectories of the swimmers. However, we do not expect that these changes affect the overall features of the flow.

B. Asymptotic states for many swimmers

As anticipated from the linear stability analysis of the single-swimmer trajectories, one observes qualitatively different behavior for small, intermediate, and large values of γ.

For small values of γ swimmers in a logarithmic potential behave essentially like a classical gas of hard-core particles [Fig. 3(a)]. We characterize the motion of the swimmers in the following by discussing the statistics of their *azimuthal velocity* L_v relative to the surrounding water

$$L_{v;i}=(\mathbf{x}_i\times\mathbf{v}_i)_z/r_i. \tag{16}$$

For small γ it amounts to a Maxwellian velocity distribution with variance 0.5. Assuming approximate isotropy of the velocity distribution one expects $\langle v^2\rangle\simeq 2\langle L_v^2\rangle$ such that this

finding implies $\langle v^2 \rangle = 1$. Hence, the width of the distribution is in line with fixing the expectation value of the velocity to unity by the self-propulsion and the choice of the dimensionless velocity scale. We will call this regime a *Maxwell cloud*.

For intermediate values of γ the swimmers arrange into a *vortex*. Our picture of vortex formation is that the self-propulsion is sufficiently strong in this regime to let individual swimmers relax rapidly to circular motion, and that head-on collisions will then rapidly mix up the systems until it finds itself in a state where all swimmers move around the center of the potential with the same sense of orientation. In that situation, however, the collisions take place with almost parallely aligned velocities. Eventually, their radial velocity almost vanishes, and they all circle around the center of the potential with azimuthal velocity sharply peaked around a value of either all $L_{v;i} = +1$ or all $L_{v;i} = -1$. Our choice to concentrate on the distribution of the azimuthal velocity was motivated by the observation that this distribution, rather than for instance the one of angular momentum, varies more strongly between the one for a vortex and the adjacent small γ and large γ states.

For large γ the vortex disintegrates. If γ is too large, stronger forces are needed to bend the trajectories of the swimmers toward the attracting center, and the persistence in the direction of the trajectories becomes very strong. As a consequence straight ballistic flights and collisions generate so much noise in the dynamics that no stable vortex is formed any more. In this state the radial velocity of most swimmers remains very small, and their motion is often highly correlated with swimmers in the immediate neighborhood. However, at each instant of time one observes a few of them moving in a clockwise direction while others move in a counterclockwise direction. Altogether this amounts to a symmetric bimodal distribution of L_v with sharp maxima at ± 1. Azimuthal velocities with a modulus larger than one are very rare in this regime because the self-propulsion fixes the total velocity to be (essentially equal to) unity. The broad background between -1 and $+1$ arises from swimmers which reverse the orientation of their motion around the center.

C. Formation of vortices

A vortex can be distinguished from a disordered state by observing that the average of L_v over all swimmers

$$\langle L_v \rangle = N^{-1} \sum_{i=1}^{N} L_{v;i}, \tag{17}$$

is very small in the disordered states at small and large γ, while it takes values close to ± 1 for a vortex. To observe how a vortex is formed we prepared systems with random initial conditions obeying $\langle L_v \rangle \simeq 0$, and followed the temporal evolution of $\langle L_v \rangle$.

Already systems with as few as five swimmers tend to arrange into stable vortexlike motion (Fig. 4). However, the time to form the vortex varies considerably for different initial conditions. Typically, the formation time never exceeds about 600 time units in a harmonic potential, and about 300 in the logarithmic potential. This time corresponds to a few tens of revolutions around the center.

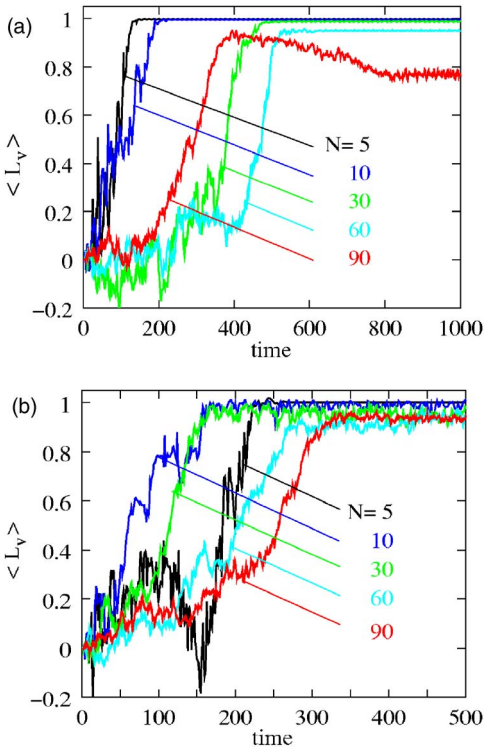

FIG. 4. (Color online) Evolution of the average azimuthal velocity $\langle L_v \rangle$ for $\gamma = 0.4$ and different numbers of swimmers for (a) the harmonic and (b) the logarithmic potential. Initially, the swimmers are arranged randomly with zero velocity. Eventually about half of the systems organize into either clockwise or counterclockwise vortexlike motion. Since the systems are otherwise statistically equivalent, the azimuthal velocity has in case been reflected so that eventually always counterclockwise motion is approached.

Both orientations of the vortex are equally likely. *A priori* it is also not excluded that a vortex reverses its orientation. For very few swimmers, this is occasionally observed, but already for 10–15 swimmers fluctuations that lead to a reversal of the orientation virtually never occur in the time interval of length $\Delta t = 50\,000$. One of these exceptional events occurred in the run for $N = 55$ in Fig. 5 (bottom right).

D. Vortices in the harmonic potential

For $\gamma = 0$ we are dealing with a system of many swimmers with short-range repulsion, which are bound in a harmonic external potential. A gas of classical particles without self-propulsion in a trapping potential also forms a vortex: due to conservation of angular momentum any angular momentum present initially will give rise to a strong vortex when the particles are attracted toward the center. As shown in Sec. III B this is no longer true for swimmers. Their self-propulsion $\gamma(1 - v^2 \mathbf{v})$ breaks conservation of angular momentum. As a consequence, at any finite value of γ the motion of swimmers is not confined to a constant angular-momentum shell. Active motion with a very small γ rather leads to a decay of the angular momentum with a rate proportional to γ. In the long run one (almost) always encounters the state occupying the largest fraction in the phase

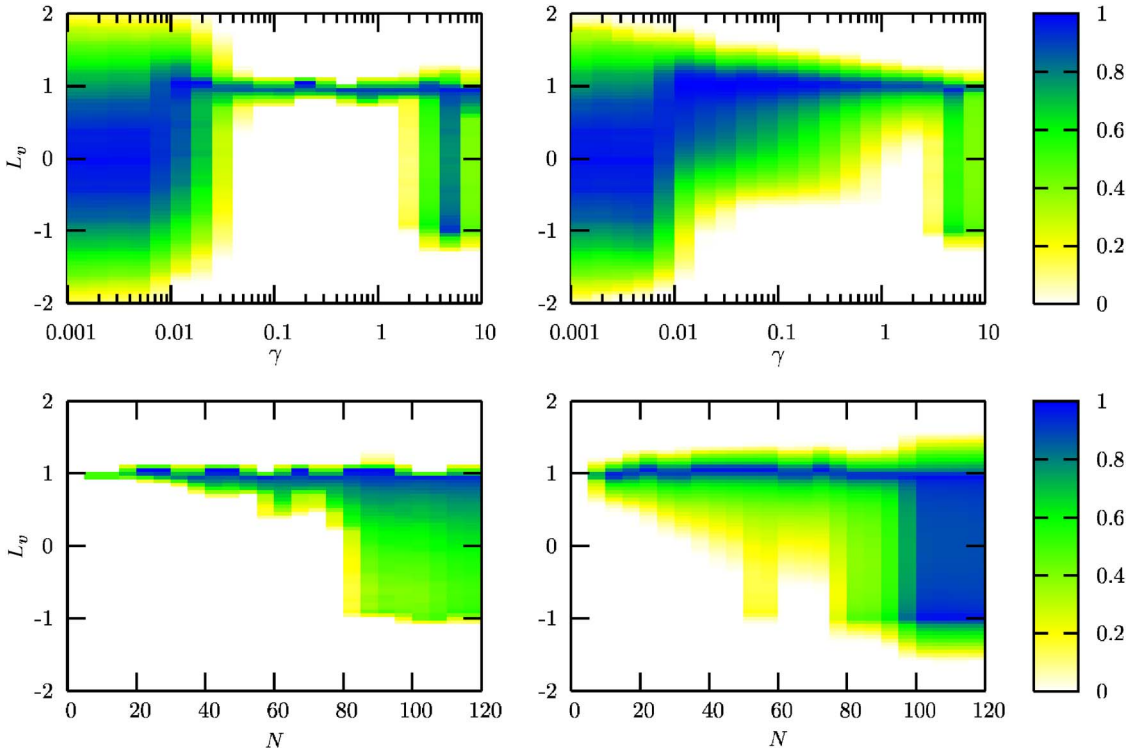

FIG. 5. (Color online) Probability distributions of azimuthal velocities L_v. The distributions have been calculated based on the time interval $1000 < t < 50\,000$, and are normalized such that the maximum of the distribution is unity. Some representative transients for the evolution of the expectation value $\langle L_v \rangle$ over all swimmers were shown in Fig. 4. The color reflects the density as indicated with the color bars to the right. It is the same for all frames. The upper left panel shows distributions for $N=40$ swimmers in a harmonic potential for different values of the restoring parameter γ. For small values of γ the distribution is centered at zero and fairly wide. Near $\gamma \simeq 0.3$ it collapses to a sharply peaked distribution around 1, indicating the formation of a vortex. Using a symmetry of the equations of motion, vortices with opposite rotation were reflected into counterclockwise rotating ones. The vortices disappear for $\gamma > 5$. The bimodal distribution of azimuthal velocities reflects that at any instant of time there are clockwise and counterclockwise rotating swimmers in the system. The lower left panel shows $\langle L_v \rangle$ distributions for fixed $\gamma=1$ as a function of the number of swimmers. For $N \lesssim 90$ there always is a vortex. For large N the vortex breaks down because of the persistence of the motion of the particles (cf. the main text). The panels on the right-hand side show the corresponding plots for the logarithmic potential. Vortices form when γ exceeds $\simeq 0.01$. However, for values of γ slightly above the transition the distribution is much broader as compared to the harmonic case. For $\gamma \gtrsim 8$ and $N \gtrsim 80$ the distributions again become bimodal, which indicates the breakdown of the vortex. For $\gamma=1$ and $N=55$ the initial conditions gave rise to a vortex which changed its orientation during the time interval used to calculate the histograms. This is reflected in a second maximum at $L_v=-1$.

space, i.e., a state with vanishing angular momentum, and the azimuthal velocity L_v distributed according to a Maxwell distribution with zero mean.

The formation of a stable vortex by swimmers must, on the other hand, also be linked intimately to their self-propulsion. Since the strength of the self-propulsion is controlled by the parameter γ, we expect to find a lower critical value for γ below which no vortex forms. The vortex Fig. 3(b) formed by swimmers differs from the vortex found in a system of passive particles in that its vorticity is selected by the dynamics, rather than being prescribed by the initial condition. The simulation results shown in the top left panel of Fig. 5 and in the left panels of Fig. 6 show this rather clearly.

For very small γ there is no preferred direction of the motion, and the probability distribution for the azimuthal velocities is a Maxwellian distribution centered around zero. For $\gamma \gtrsim 0.01$ the distribution tends to become asymmetric on the time scale $\Delta t = 50\,000$. Subsequently, around $\gamma=0.02$, the distribution becomes much narrower than a Maxwellian (for all $N \gtrsim 20$ the variance at $\gamma=0.1$ approaches the constant value of $\simeq 0.06$), and is centered around either +1 or −1: A vortex has formed. For $\gamma \gtrsim 2$ the vortex disintegrates again due to the frequent collisions of particles and the slow relaxation to the circular motion.

Both stability borders of the vortex are in line with the results of the linear stability analysis in Fig. 2(○). For $r_* \simeq 3 \cdots 4$, which is the typical size of the vortex for the number of particles considered here, the parameter range, where we find vortices amounts to $0.1 \lesssim \gamma r_* \lesssim 10$, which is right in the center of the region where the circular motion is most stable.

An additional interesting finding is that vortices arising for large numbers of swimmers have an almost rigidly rotating core, where the neighbor relations between swimmers are preserved. Intuitively, this behavior can be understood by observing that confinement of interacting swimmers in a harmonic potential creates a pressure in the center which increases rapidly with the number of swimmers. This leads to the formation of a solidlike phase where the neighbors of the swimmers remain the same for long stretches of time.

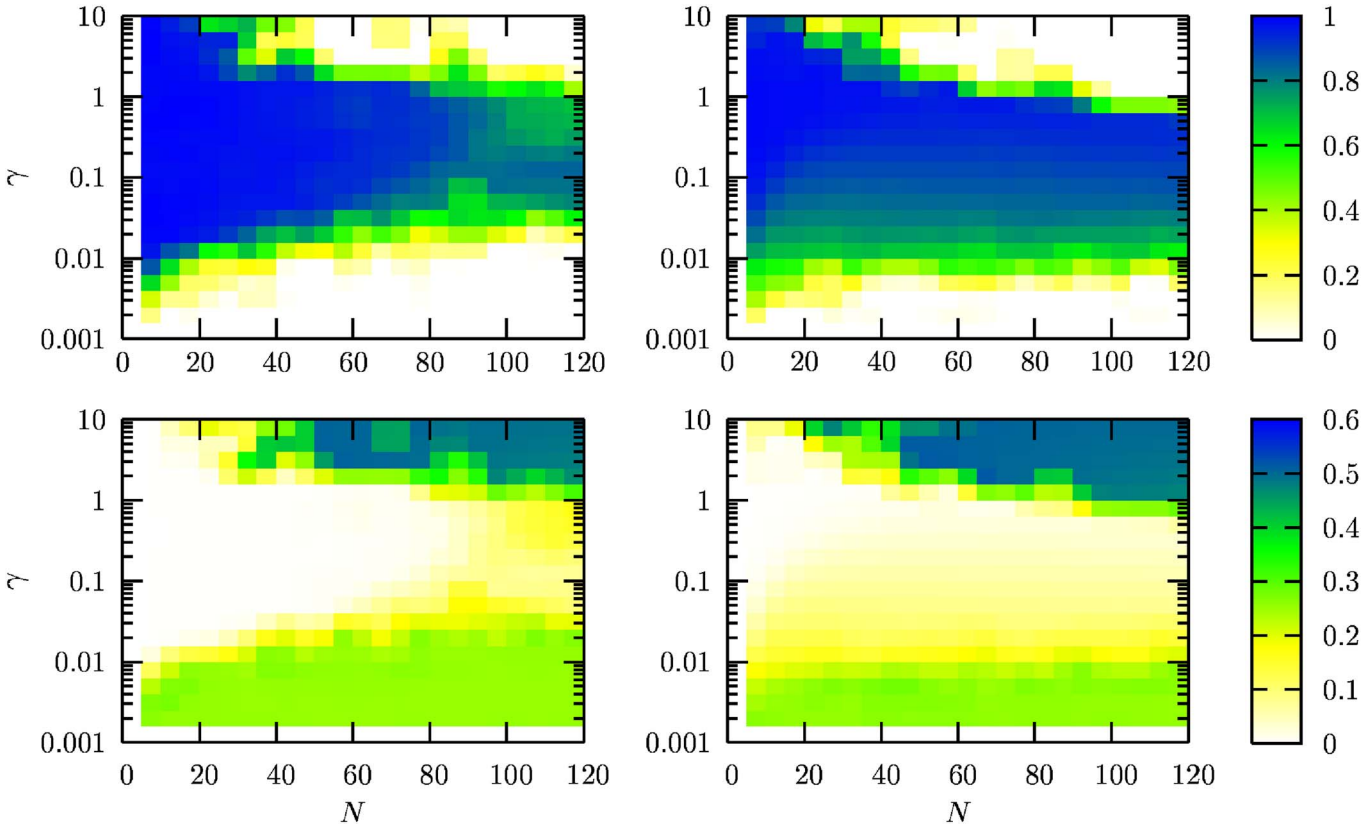

FIG. 6. (Color online) Mean (top) and variance (bottom) of the distributions of L_v. The left and right panels again refer to motion in a harmonic and logarithmic potential, respectively. Figure 5 shows the full distributions for sections through these diagrams at fixed N (Fig. 5, top) and γ (Fig. 5, bottom), respectively. In the upper diagrams dark colors (blue) indicate regions with a vortex where the mean value is close to unity. For the Gaussian-like distribution for small γ and the bimodal one at large γ the mean is close to zero (white). When the vortex is formed the distribution tends to be very narrow. This is shown in the lower diagrams, where the vortex appears in light colors, while the much broader distributions at large and small γ are dark (green and blue).

When a vortex is formed the probability distribution to find a swimmer with L_v is centered around either +1 or −1 rather than around 0 (Fig. 5, left panels). Moreover, the L_v distribution is much narrower for a vortex than in the case of disordered motion. In view of this the phase boundaries in the $N-\gamma$ plane can be identified by plotting the first or second moment of the distribution in this parameter plane (Fig. 6, right panels). When the number of swimmers substantially exceeds 100 the vortex disintegrates due to the strong pressure built up by the strong confinement of the swimmers in the potential. For $N \lesssim 100$ very stable vortices are formed in a γ range between 0.1 and 1. As estimated above this range matches nicely with the range of parameters in the linear stability analysis for which the circular motion is the most stable. For decreasing particle numbers the region increases because there are fewer interactions per unit time which could break up the vortex.

E. Vortices in the logarithmic potential

In accordance with the stability analysis vortices form in a logarithmic potential for a similar range of γ values as in the harmonic case [right panels of Figs. 5 and 6]. Also in this case the first and second moment of the distribution of L_v exhibit a very sharp transition when a vortex is formed (Fig. 6, right panels). Irrespective of the number of swimmers N the vortex is formed for $\gamma \gtrsim 10^{-3}$, and it disintegrates when γ exceeds unity. We encounter hysteresis and find regions of bistability close to the upper transition region, where the formation of the vortex can take very long—occasionally up to ten times longer than far away from the boundary. For the upper boundary, repeated simulations with different initial conditions indicate that there is an extremely broad coexistence region of vortex and disordered states. For $N=50$ it ranges between about $\gamma=0.5$ and 5.

Provided that a vortex containing all swimmers fits into the container without interfering with the walls these findings remain the same irrespective of the size of the container. Eventually the interaction with the confining wall leads to a breakdown of vortex formation when the number of swimmers is increased at a fixed size of the container. For instance, for the systems bounded by a container of radius 10 frequent collisions with the wall destroy the vortex when the number of swimmers exceeds about 80.

IV. CONCLUDING REMARKS

We have discussed swimmers in the presence of a potential mimicking an attraction to a center, as it has been ob-

served in the motion of *Daphnia magna* in response to a light beam.

For a harmonic confining potential the attractive forces become very large far away from the center such that all swimmers will approach a region close to the light beam. This potential therefore does not reproduce the experimental finding that a vortex close to the light beam is always surrounded by a fairly constant low density of swimmers far away. Moreover, the accumulation of swimmers close to the center leads to a freezing of nearest-neighbor relations in the azimuthal direction when the number of swimmers is increased.

On the other hand, a logarithmic potential can stabilize circular motion of arbitrary radius with a constant prescribed speed. A slightly stronger force gives rise to a preferred radius, but if the increase is weak, the restoring force in the radial direction is only weak and the ever present fluctuations in their motion due to their mutual interaction can distribute the swimmers over a wide radius. The simulations show that the swimmers participating in the vortex are not fixed: swimmers can enter and leave the vortex region, depending on their mutual interactions and their direction of motion. It will be interesting to study the rate of exchange of swimmers in the vortex and in the surrounding fluid.

We emphasize in this respect that the present model does not have an explicit external source of noise. The fluctuations are all self-generated through the short-range repulsive swimmer-swimmer interactions. In view of this the nonequilibrium phase transitions described in the present work differ substantially from those discussed in [21,25,26,29], where there are no repulsive interactions and the transitions are induced by varying the strength of an external white noise in the equations of motion.

For an experimental test of the attractive potential, vortex forming insects might also be suited. Swarming insects in air induce a weaker fluid flow than *Daphnia*, so that the distribution of their peculiar velocities can more easily be separated from the motion of the medium they move in.

Our main result is to highlight the constructive and destructive role of the self-propulsion for the formation of the observed vortices. Without self-propulsion angular momentum is preserved and a vortex can only arise from a concentration of an angular momentum initially present. On the other hand, if self-propulsion is too strong, straight line motion persists, and swimmers escape from the potential. This dual role is reflected in a lower and upper limit to the range of γ values in which a vortex forms. The formation of the vortex can conveniently be identified based on the distribution of the azimuthal velocity which is broad and symmetric around zero when no vortex is formed, and very sharply peaked around $+1$ or -1 for a vortex. The transitions between the states were explained based on a linear-stability analysis of individual trajectories. It shows that the asymptotic circular motion becomes unstable against a small perturbation for both small and large values of γ. In this respect the motion in the presence of an attractive force to a center appears to be different from the situation where swarms are formed in spatially uniform systems. After all, the latter systems even show formation of swarms when only the direction of their velocity is changing, but its modulus is fixed. (Formally this would amount to the limit $\gamma \to \infty$.) From the point of view of the classification of their phase transitions the vortices formed in reaction to attractive forces between the swimmers and vortices arising in reaction to an external stimulus therefore apparently fall into different universality classes.

ACKNOWLEDGMENTS

This work was partially supported by the Deutsche Forschungsgemeinschaft. We thank Anke Ordemann and Frank Moss for generously sharing their insights into the behavior of *Daphnia Magna*, and Tobias M. Schneider for discussions on the linear-stability analysis and for comments on the manuscript.

[1] M. Resnick, *Turtles, Termites, and Traffic Jams* (MIT Press, Cambridge, 1994).
[2] E. Ben-Jacob, I. Cohen, and H. Levine, Adv. Phys. **40**, 395 (2000).
[3] C. W. Reynolds, Comput. Graph. **21**, 25 (1987).
[4] J. K. Parrish and L. Edelstein-Keshet, Science **284**, 99 (1999).
[5] G. Flierl, D. Grünbaum, S. Levin, and D. Olson, J. Theor. Biol. **196**, 397 (1999).
[6] I. D. Couzin and J. Krause, in *Advances in the Study of Behavior* edited by P. Slater, J. Rosenblatt, C. Snowdon, and T. Roper (Elsevier, New York, 2003), Vol. 32, pp. 1.
[7] M. Collett, E. Despland, S. J. Simpson, and D. C. Krakauer, Proc. Natl. Acad. Sci. U.S.A. **95**, 13052 (1998).
[8] J. Deneubourg, A. Lioni, and C. Detrain, Biol. Bull. **202**, 262 (2002).
[9] S. Gueron, S. Levin, and D. I. Rubenstein, J. Theor. Biol. **182**, 85 (1996).
[10] H. E. Stanley, *Introduction to Phase Transitions and Critical Phenomena*, International Series of Monographs on Physics (Oxford, New York, 1987).
[11] J. J. Binney, The Theory of Critical Phenomena: An Introduction to the Renormalization Group (Clarendon Press, Oxford, 1995).
[12] T. Vicsek, A. Czirók, E. Ben-Jacob, I. Cohen, and O. Shochet, Phys. Rev. Lett. **75**, 1226 (1995).
[13] A. Czirók, H. E. Stanley, and T. Vicsek, J. Phys. A **30**, 1375 (1997).
[14] J. Toner and Y. Tu, Phys. Rev. Lett. **75**, 4326 (1995).
[15] J. Toner and Y. Tu, Phys. Rev. E **58**, 4828 (1998).
[16] G. Grégoire, H. Chaté, and Y. Tu, Phys. Rev. E **64**, 011902 (2001).
[17] H. Levine, W.-J. Rappel, and I. Cohen, Phys. Rev. E **63**, 017101 (2001); localized flock of finite extent, vortex solution.
[18] F. Schweitzer, W. Ebeling, and B. Tilch, Phys. Rev. Lett. **80**, 5044 (1998).
[19] W. Ebeling, F. Schweitzer, and B. Tilch, BioSystems **49**, 17

(1999).
[20] U. Erdmann, W. Ebeling, F. Schweitzer, and L. Schimansky-Geier, Eur. Phys. J. B **15**, 105 (2000).
[21] U. Erdmann, W. Ebeling, and V. S. Anishchenko, Phys. Rev. E **65**, 061106 (2002).
[22] J. K. Parrish, S. V. Viscido, and D. Grünbaum, Biol. Bull. **202**, 296 (2002).
[23] G. Grégoire, H. Chaté, and Y. Tu, Physica D **181**, 157 (2003).
[24] G. Grégoire and H. Chaté, Phys. Rev. Lett. **92**, 025702 (2004).
[25] A. S. Mikhailov and D. H. Zanette, Phys. Rev. E **60**, 4571 (1999).
[26] U. Erdmann, W. Ebeling, and A. S. Mikhailov, Phys. Rev. E **71**, 051904 (2005).
[27] R. Mach and F. Schweitzer, in *Advances in Artificial Life*, Lecture Notes in Artificial Intelligence (LNAI), edited by W. Banzhaf, T. Christaller, P. Dietrich, J. Kim, and J. Ziegler (Springer, Berlin, 2003), vol. 2801, pp. 810–820.
[28] R. Mach, A. Ordemann, and F. Schweitzer, q-bio.PE/0404028.
[29] W. Ebeling, J. Dunkel, U. Erdmann, and S. Trigger, J. Phys.: Conf. Ser. **11**, 89 (2005).
[30] A. Ordemann, The Biological Physicist **2**, 5 (2002).
[31] A. Ordemann, G. Balázsi, and F. Moss, Physica A **325**, 260 (2003a).
[32] A. Ordemann, F. Moss, and G. Balázsi, Nova Acta Leopold. **332**, 87 (2003b).
[33] L. Turner, W. S. Ryu, and H. C. Berg, J. Bacteriol. **182**, 2793 (2000).
[34] W. Ebeling and F. Schweitzer, Theory Biosci. **120**, 207 (2001).
[35] W. Ebeling and G. Röpke, Physica D **187**, 268 (2004).
[36] A. Ordemann (private communication).
[37] One could also obtain a length from v_0 and γ_0, but this would complicate studies with varying γ_0.